processes

MDPI

Article

Surface Subsidence Characteristics of Mining Panel Layout Configuration with Multi-Seam Longwall Mining

Hengzhong Zhu [1,2,3,*], Huajun Wang [4], Rong Gao [5] and Yongqiang Zhao [1]

[1] State Key Laboratory of Water Resource Protection and Utilization in Coal Mining, Beijing 102209, China
[2] School of Energy and Mining Engineering, Shandong University of Science and Technology, Qingdao 266590, China
[3] State Key Laboratory of Strata Intelligent Control and Green Mining Co-Founded by Shandong Province and the Ministry of Science and Technology, Shandong University of Science and Technology, Qingdao 266590, China
[4] School of Mining and Mechanical Engineering, Liupanshui Normal University, Liupanshui 553000, China
[5] Energy Administration of Zhijin County, Bijie 552100, China
* Correspondence: skd996317@sdust.edu.cn

Abstract: Mining-induced subsidence is critical for ecological environment reconstruction and damage prevention in coal mining areas. Understanding the characteristics of surface subsidence with multi-seam mining is the first step. Surface subsidence of different mining panel layout configurations was investigated by means of UDEC numerical simulation. Based on the simulation results, it was indicated that mining panel layout configuration had a significant impact on surface subsidence, including ground surface subsidence, horizontal displacement, crack propagation, and ground surface fissure development. The overlapped region of the upper panel and the lower panel is the key region, where existing bedding separations and strata cracks close and activate, the integrity and strength of the interburden layer are reduced, and the subsidence magnitude is enhanced. The subsidence profile of the overlapped region for the stacked configuration, external staggered, the edge of the lower panel internal staggered, two edges of the lower panel internal staggered are steeper and deeper, and the corresponding values of ground surface subsidence and horizontal displacement are greater than other regions. The ground surface fissures with the types of stepped, slided, and graben developed on the ground surface above the edge of the mining panel, and the development location is closely related to the strata movement edge. Because of the support activities of the reserved coal pillar, the ground subsidence of the external staggered (internal staggered) of the upper panel with the coal pillar is slight. The external staggered (internal staggered) and external staggered (internal staggered) of the upper panel with the coal pillar can be selected as the preferred layout configuration. The proposed description of surface subsidence of different mining panel layout configurations can be applied in subsidence prediction.

Keywords: multi-seam surface subsidence; mining panel layout configuration; numerical simulation; ground surface movement; ground surface fissure development

Citation: Zhu, H.; Wang, H.; Gao, R.; Zhao, Y. Surface Subsidence Characteristics of Mining Panel Layout Configuration with Multi-Seam Longwall Mining. *Processes* **2023**, *11*, 1590. https://doi.org/10.3390/pr11061590

Academic Editor: Guining Lu

Received: 21 March 2023
Revised: 17 May 2023
Accepted: 20 May 2023
Published: 23 May 2023

1. Introduction

Mining-induced surface subsidence (MISS) has been increasingly recognized as a key issue due to the increase in the intensity of coal seam resources, which is known to be a source of damage to buildings, plows, grasslands, forests, water resources, etc. [1–3]. Due to the urgent need for ecological mine construction, the prediction of the effects of underground coal mining on the ground surface is essential for coal mining companies. In comparison with single-seam mining, multi-seam surface subsidence includes profile, shape, and magnitude and presents distinct strata movement features.

Multiple published reports have explained surface subsidence from various perspectives [4,5]. Regarding theoretical studies, early studies on mining subsidence originated in

Belgium. In 1825, a relevant investigation on the surface damage of Liege City proved that the surface damage was mainly caused by mining operations within a depth of 90 m, and mining depth played a decisive role in surface damage [6]. The "perpendicular theory" and "normal theory" about mining-induced damage were proposed [7–9]. In 1919, Lehmann proposed the "sinking basin" theory, using the ground surface strain to represent the compression and tension deformation in longwall mining [10]. It is believed that the subsidence profile shows an upward trend in the tension area and a downward trend in the compression area. In 1928, Keinhurst first proposed a calculation method for mining-induced subsidence division [11]. In 1947, Avershin published the book "*Rock strata movement in underground coal mining*", and proposed the famous viewpoint that "horizontal movement is proportional to ground surface tilt" [12]. Perz incorporated a time factor into the subsidence calculation formula, which led to the development of surface subsidence as a dynamic process rather than static process [13]. After 1950, Knothe proposed the normal distribution influence function based on actual observation, which is a widely used method for predicting surface subsidence [14]. Litwiniszyn regarded rocks as discontinuous media and proposed the random media theory [15]. Until now, the Knothe influence function (1951), random media theory (1954), and probability integral method (1965) have been widely applied [16]. Afterward, the continuum theory, the geometric theory, the theory of different boundary states, and the surface element theory were also promoted [17].

It has been indicated that the MISS characteristics are closely related to coal seam properties, coal seam mining factors, ground surface features, and interburden properties [18,19]. Various prediction models for surface subsidence have been obtained. A time function model that includes mining parameters, geological parameters, and grout injection parameters for assessing the dynamic surface subsidence of grout-injected overburden was established [20]. An analogous hyperbola subsidence model to describe the inner burden movement and the bulking factor was proposed to predict surface subsidence [21]. In addition, the analogous hyperbola, analogous hyperbola-funnel, and analogous funnel models were described to predict surface subsidence under the inclined coal seam mining conditions [22]. A Knothe time function considering the influence coefficient of unconsolidated layers was established to improve the accuracy of surface subsidence prediction [23]. As for the surface subsidence of backfill-strip mining, a prediction method to predict the surface subsidence of backfill mining and strip mining separately was proposed [24]. The surface subsidence based on the lognormal function was also established from the view of skewed subsidence features, and the relationship between wave curves and vibration curves was also determined [25]. Taking geological characteristics and design features into account, a numerical model based on the finite element method to predict surface subsidence was raised [26]. A 3D discontinuous numerical model incorporating geological complexities and the backfilling sequence was used, and the surface subsidence profile was obtained [27]. Under the condition of deep pillarless mining, a new model to identify the initiation of subcritical subsidence was developed [28].

To date, many studies have been conducted on mining damage and surface deformation. For example, the damage characteristics and the transmission mechanism of overlying rock strata were analyzed, and evaluated the forms of surface damage [29]. Denise Müller proposed that the differences in tilt subsidence or horizontal changes in length should be preferred to describe the relevance of mining damage on buildings [30]. Interferometric synthetic aperture radar (InSAR) time series analysis was applied to assess the amount of damage above coal mining areas, and a model of the relationship between the damage level to constructions and ground deformation due to mining damage was developed [31]. The method combining subsidence theory and slope stability analysis was also proposed for building damage assessment in mountainous mining damage areas [32]. The fuzzy set theory was applied to evaluate and rank mining damage prevention [33]. Regarding the frameworks on surface subsidence, ALPRIFT, a new framework, was introduced for mapping subsidence vulnerability indices. The ALPRIFT framework for subsidence comprises seven data layers: Aquifer media (A), Land use (L), Pumping of groundwater, Recharge (R),

Aquifer thickness Impact (I), Fault distance (F), and Decline of Water Table (T) [34]. Based on the ALPRIFT framework, the Dynamic Subsidence Vulnerability Index (DSVI) was introduced to estimate possible land subsidence time variations by considering changes in groundwater level [35]. Subsidence vulnerability indexing (VI) was transformed into risk indexing (RI) using a new fuzzy-catastrophe scheme based on ALPRIFT [36]. Additionally, inclusive multiple modeling (IMM), which combines two common approaches of multi-criteria decision-making (MCDM) at Level 1 and artificial intelligence (AI) at Level 2, was also presented [37].

It has been indicated that the surface subsidence of multi-seam mining has its own special features [38]. After the upper panel has been mined out, the overburden strength is reduced due to separation and fissure development, then the magnitude of multi-seam mining increases; correspondingly, the MISS profile becomes deeper and steeper above the region of overlapped panels [39]. Existing studies have observed that the surface subsidence profile and magnitude significantly depend on the mining panel layout configuration [40,41]. The magnitude of incremental multi-seam surface subsidence even exceeds the thickness of the mining panel [42]. The movement angle of multi-seam mining was observed to be greater than single-seam mining [43]. Additionally, the maximum incremental subsidence value was not generated above the middle section after the mining panel was extracted [44]. Compared with single-seam surface subsidence, the multi-seam subsidence differences can be described as subsidence factor changes, the surface subsidence profile changes, and the crack angle or movement angle changes [45,46].

However, there have been a few specialized studies on MISS aiming at different mining panel layout configurations. The overlapped extent, relative location, and interburden thickness of mining panels can be presented as mining panel layout configurations. Compared with prevention measures after the surface subsidence emerges, the mining layout configuration is the fundamental measure from the source to reduce the adverse effects of surface subsidence before it occurs. The ground surface subsidence degree of different mining layout configurations was obtained, and the preferred layout configuration can be selected. In engineering practice, the specific layout configuration can be determined to reduce the adverse effects on the ground surface environment.

This study reveals the surface subsidence characteristics of different mining panel layout configurations. In this study, numerical simulation was used for this purpose. In the numerical model, geological parameters such as rock mass properties, coal seam properties, and extraction thickness were kept constant. This enabled the study of the surface subsidence characteristics under the influence of mining panel layout configurations. Eight different mining panel layout configurations and their corresponding numerical results were compared. After a comparison of vertical displacement, horizontal displacement, subsidence coefficient, and ground fissure development, the preferred layout configuration can be determined to reduce MISS from the source.

2. Mining Panel Layout Configuration

Significantly different from the treatment measures after MISS development, the deployment of mining panels is a reduction control measure for MISS. Different mining panel layout configurations have specific effects on MISS, which is an important factor affecting the degree of MISS development. According to abundant field observations and combined with the width of mining panels, mining panel layout configurations were summarized as follows. The length of the upper and lower panel is based on field investigation. In China, the length of a mining panel is generally 100–240 m. When the coal seam thickness is greater than 3.5 m, the length of a mining panel is usually greater than 200 m. When the coal seam thickness is less than 3.5 m, the length of a mining panel is usually between 120 m and 200 m. Regarding our study, the thickness of the upper seam and the lower seam were 2 m and 3 m, respectively. Hence, 120 m and 180 m were selected as the width of the mining panels.

2.1. Mining Panel Layout Configuration with Equal Width

Supposing the width of the upper panel and the lower panel are equal, according to the relative location of the panels in two seams, the mining panel layout configuration with equal width can be divided into stacked, external staggered, and internal staggered. A detailed description can be expressed as follows: (1) Stacked, the edges of the upper panel and the lower panel are vertically aligned (Figure 1a); (2) External staggered, the edges of the upper panel and the lower panel are not aligned, and the upper panel is staggered outside the lower panel with a certain width (Figure 1b); (3) Internal staggered, the edges of the upper panel and the lower panel are also not aligned, and the upper panel is staggered inside the lower panel with a certain width (Figure 1c).

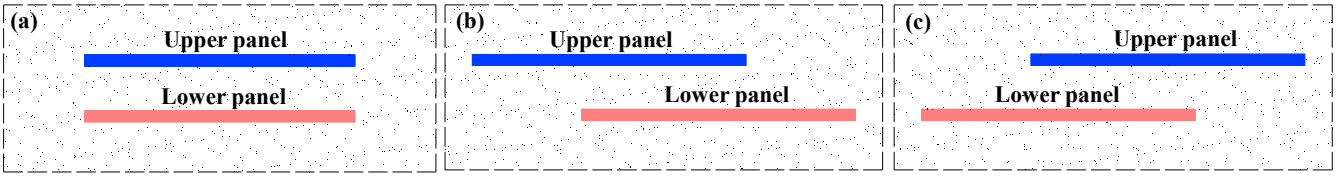

Figure 1. Mining panel layout configurations with equal width: (**a**) stacked; (**b**) external staggered; (**c**) internal staggered.

2.2. Mining Panel Layout Configuration with Unequal Width

Supposing the width of the upper panel and the lower panel are unequal, according to the relative location of the panels in two seams, the mining panel layout configuration with unequal width can be divided into: (1) The edge of the upper panel internal staggered: the width of the upper panel is less than the lower panel, one edge of the upper panel and the lower panel is vertically aligned, and the other edge of the upper panel is internally staggered with the lower panel by a certain width (Figure 2a); (2) The edge of the lower panel internal staggered: the width of the lower panel is less than the upper panel, one edge of the upper panel and the lower panel is vertically aligned, and the other edge of the lower panel is internally staggered the upper panel by a certain width (Figure 2b); (3) Two edges of the upper panel internal staggered: the width of the upper panel is less than the lower panel, two edges of upper panel are internally staggered with the lower panel (Figure 2c); (4) Two edges of the lower panel internal staggered: the width of the upper panel is greater than the lower panel, two edges of lower panel are internally staggered with the upper panel (Figure 2d).

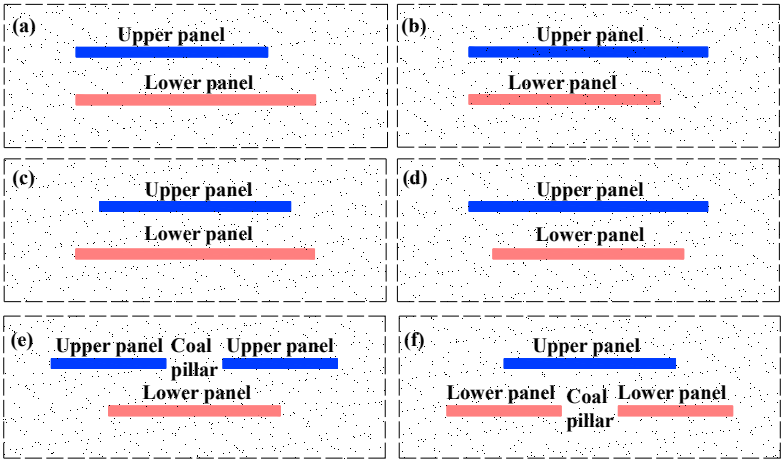

Figure 2. Mining panel layout configurations with unequal width: (**a**) the edge of the upper panel internal staggered; (**b**) the edge of the lower panel internal staggered; (**c**) two edges of the upper panel internal staggered; (**d**) two edges of the lower panel internal staggered; (**e**) external staggered of the upper panel with a coal pillar; (**f**) internal staggered of the upper panel with a coal pillar.

When a coal pillar is reserved, the mining panel layout configuration can be divided into external staggered with a coal pillar and internal staggered with a coal pillar. (1) External staggered of the upper panel with coal a pillar, the upper panel is divided into two sections, with a certain width of coal pillar reserved between them. The width of the upper panel is greater than that of the lower panel, and two edges of the lower panel are internally staggered with the upper panel (Figure 2e); (2) Internal staggered of the upper panel with coal a pillar, the lower panel is divided into two sections, with a certain width of coal pillar reserved between them. The width of the lower panel is greater than that of the upper panel, and the two edges of the upper panel are internally staggered with the lower panel (Figure 2f).

3. Surface Subsidence Characteristics of Mining Panel Layout Configuration

3.1. Numerical Model

To clarify the surface subsidence of different mining panel layout configurations, a numerical simulation model was established using UDEC discrete element software. The numerical simulation model takes mining panels of the Jiaozishan coal mine as the research background. Jiaozishan coal mine is located in Guizhou province, Southwestern China. The thickness of the upper seam and the lower seam were 2 m and 3 m, respectively, and the interburden thickness was 21 m. The model is 200 m in length and 59∼106 m in height, with the bottom boundary fixed in the vertical direction and the side boundary fixed in the horizontal direction (Figure 3).

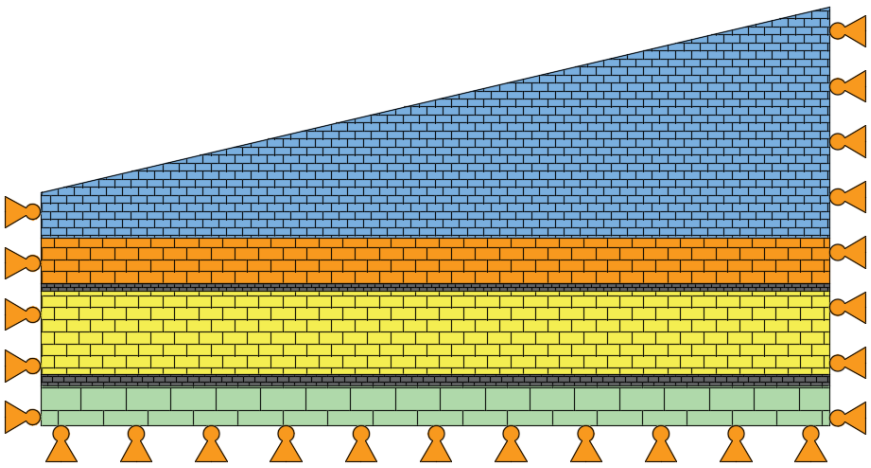

Figure 3. The numerical simulation model.

The Mohr–Coulomb yield criterion was used for the model, and Coulomb slip with surface contact was used for the joint material model. The calculation process can be expressed as follows: initial stress field balance → upper panel extraction → lower panel extraction. After the model was established, the numerical simulation procedure can be divided into three steps: (1) according to the burial depth of the upper coal seam and lower coal seam, the initial stress was applied on the top of the model so as to obtain the initial stress equilibrium state of the model. (2) The excavation of the upper and lower coal seam was simulated by a null model; each excavation distance was 10 m. In order to obtain monitoring data on vertical displacement and horizontal displacement, the monitoring point was arranged along the surface of the model. (3) Based on monitoring data on vertical and horizontal displacement, the surface subsidence profile was obtained, and then the surface subsidence degree of different mining panel layout configurations can be compared.

The immediate roof is siltstone, the main roof is limestone, the overlying strata are fine sandstone, and the floor is mudstone. Based on the laboratory test results of the rock mass sample and combined with the relevant studies, the rock mass parameters for numerical simulation were obtained (Tables 1 and 2).

Table 1. Physical and mechanical parameters of coal and rock mass.

Rock Strata	Density (kg·m^{-3})	Bulk Modulus /GPa	Shear Modulus /GPa	Tensile Strength /MPa	Cohesion /MPa	Friction Angle /(°)
Overlying strata	2400	4.0	3.0	3.0	2.8	27
Main roof	2550	6.9	4.5	4.4	5.5	38
Immediate roof	2100	3.0	1.3	2.0	2.5	26
Coal seam	1400	1.7	1.0	1.4	1.6	20
Floor	2650	6.6	4.0	3.7	3.2	30

Table 2. Joint mechanics parameters of coal and rock mass.

Rock Strata	Normal Stiffness /GPa	Shear Stiffness /GPa	Tensile Strength /MPa	Cohesion /MPa	Friction Angle /(°)
Overlying strata	4.0	2.5	0	0.10	17
Main roof	7.0	3.0	0	0.03	20
Immediate roof	3.0	1.5	0.04	0.02	14
Coal seam	2.0	1.0	0	0.05	12
Floor	10	8.0	1.0	0.12	20

3.2. Ground Surface Subsidence

Ground surface subsidence is an important assessment index that can be used to evaluate the degree of ground surface damage. The ground surface subsidence of different mining panel layout configurations was obtained, as shown in Figure 4.

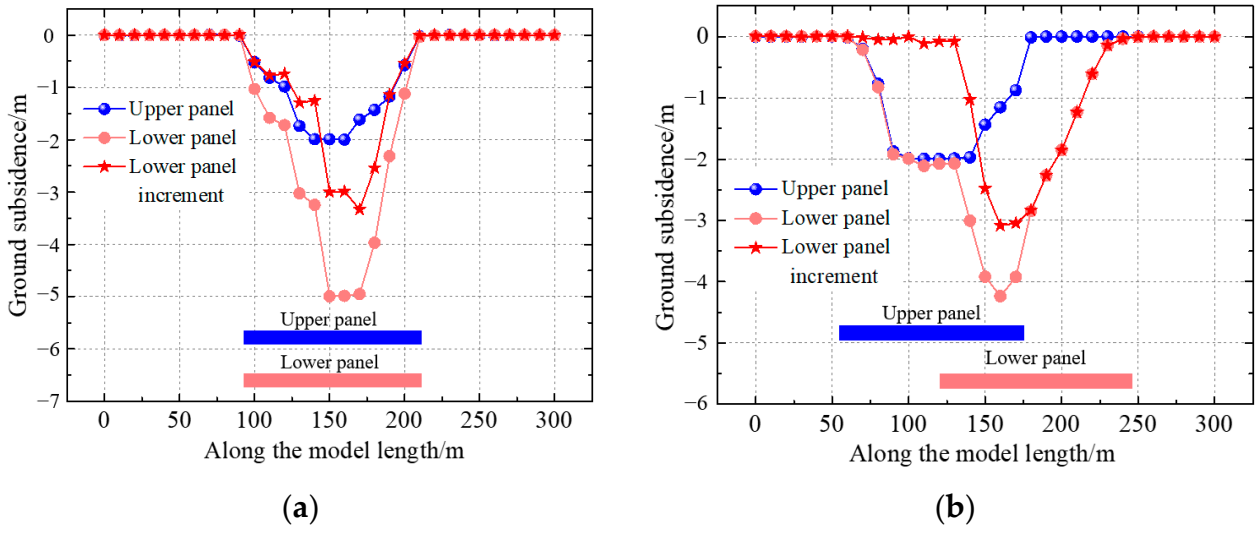

Figure 4. *Cont.*

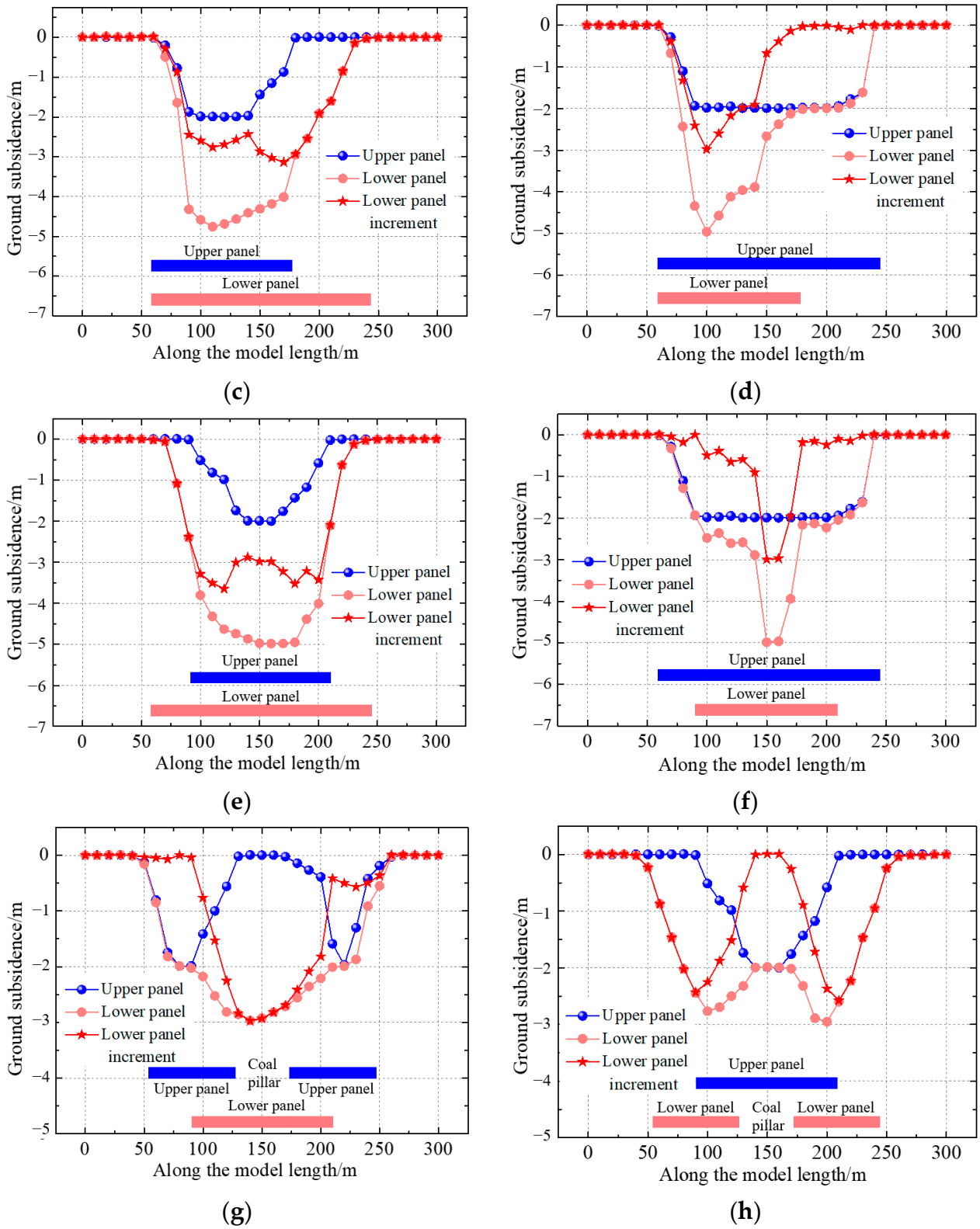

Figure 4. Ground surface subsidence of different mining panel layout configurations: (**a**) stacked; (**b**) external staggered; (**c**) the edge of the upper panel internal staggered; (**d**) the edge of the lower panel internal staggered; (**e**) two edges of the upper panel internal staggered; (**f**) two edges of the lower panel internal staggered; (**g**) external staggered of the upper panel with a coal pillar; (**h**) internal staggered of the upper panel with a coal pillar.

3.2.1. Stacked

The width of the upper panel and the lower panel was 120 m. The ground surface subsidence after the panel was extracted, as shown in Figure 4a. The maximum value of MISS was nearly −2 m; after the lower panel was extracted, it increased significantly to −5 m. MISS of the stacked region included the caved area above the goaf of the upper panel, and the interburden had an obvious superimposed effect. The profile of MISS became narrow and deep, with a steep decline at the edges of the mining panel.

3.2.2. External Staggered

MISS of the external staggered as shown in Figure 4b. After the upper panel was extracted, the maximum value of MISS was located in the middle of the goaf, while the maximum value of MISS was located on the right side of the overlapped region. In comparison to the staggered, the maximum value of MISS decreased to −4.4 m, but the MISS of the lower panel increment decreased inconspicuously.

3.2.3. The Edge of the Upper Panel Internal Staggered

The widths of the upper and lower panels were 120 m and 180 m, respectively. After the lower panel was extracted, the maximum value of MISS was not located in the middle region of the lower goaf but in the middle region of the upper goaf. The MISS of the overlapped region increased significantly, with the maximum value increasing from −2 m to −4.76 m (Figure 4c). The increase in MISS on the right side of the overlapped region was prominent, which indicated that the extraction of the lower panel not only increased the value of MISS but also expanded its range. The MISS of the external staggered region was significantly reduced, which was only due to the extraction of the lower panel.

3.2.4. The Edge of the Lower Panel Internal Staggered

After the upper panel was extracted, the MISS basin presented the shape of a plate, and the maximum value of MISS was −1.993 m. The MISS presented the subregion feature; that is, the MISS of the overlapped region was relatively large, while the MISS of the lower panel's internal staggered region was relatively small. The MISS maximum value of overlapped region achieved 4.961 m, and its distribution was on the left side of the overlapped region. Closer to the right edge of the lower panel, the MISS value decreased from the maximum value to the value with the upper panel extraction. It indicated that the closer to the external staggered region of the upper panel, the weaker the influence of MISS for the upper panel on the strata movement of the lower panel.

3.2.5. Two Edges of the Upper Panel Internal Staggered

As shown in Figure 4e, the MISS development profile presented the shape of a bowl, and the maximum value of MISS was approximately −2 m. After the lower panel was extracted, combined with the superimposed effect of surface subsidence, the MISS of the overlapped region increased significantly, and the MISS value increased to 2.39 m in the external staggered region of the lower panel. This means that the surface subsidence of the external staggered region was obviously affected by the mining-induced influence of the upper panel.

3.2.6. Two Edges of the Lower Panel Internal Staggered

The MISS profile emerged as the shape of the plate after the upper panel was extracted, while the MISS profile presented the shape of a hopper after the lower panel was extracted. The MISS value was about −2.6 m in the range of 90–120 m, along the width of the lower panel was about −2.2 m in the range of 180–210 m. These two regions were less affected by the mining-induced superimposed effect. The MISS value was nearly −5 m in the range of 130–170 m along the width of the lower panel, indicating that the range was completely affected by the mining-induced superimposed effect.

3.2.7. External Staggered of the Upper Panel with a Coal Pillar

The width of the upper panel was 180 m, divided into two sections, with a width of 40 m for the interval coal pillar. The width of the lower panel was 120 m. After the lower panel was extracted, there was no significant change in the MISS of the external staggered region for the upper panel, and its value was equivalent to the MISS after the upper panel was extracted. The significant change area of MISS was mainly in the overlapped region, and MISS also increased correspondingly. When the upper panel was extracted, the MISS value of the interval coal pillar region was small due to the cushion effect of the coal pillar. After the lower panel was extracted, the MISS value of the interval coal pillar region increased significantly. Compared with other mining panel layout configurations, the MISS value decreased significantly to −2.87 m.

3.2.8. Internal Staggered of the Upper Panel with a Coal Pillar

After the upper panel was extracted, the profile of MISS emerged in the shape of a *V*, and the maximum value was distributed in the middle region of the goaf. When the lower panel was extracted, the MISS profile presented the shape of a *W*, and the maximum value was distributed in the overlapped region. Compared with the upper panel, the maximum value increased to 2.95 m.

3.3. Horizontal Displacement

The ground surface damage was closely related to horizontal displacement and had a significant influence on ground damage, including ground fissures, collapsed holes, and mining-induced landslides [47,48]. The development profile of horizontal displacement for different mining panel layout configurations is presented in Figure 5.

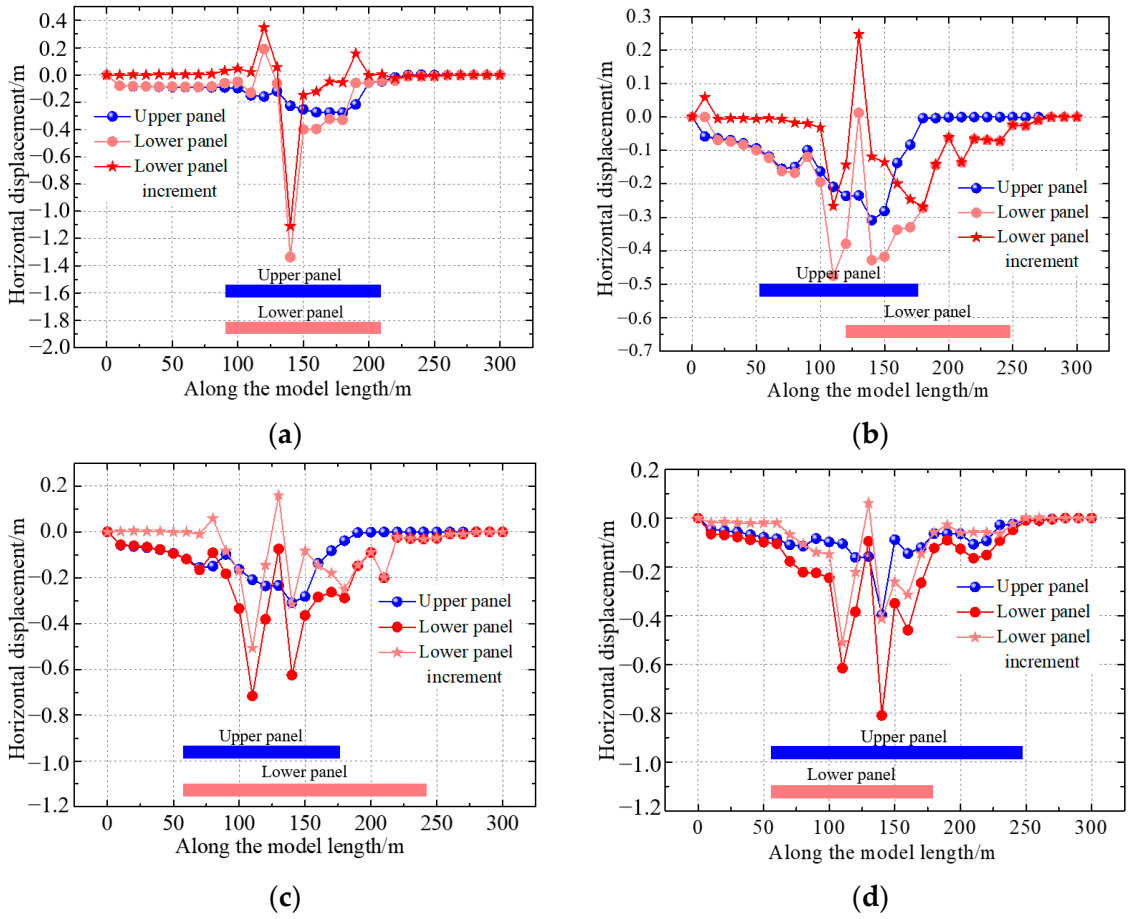

Figure 5. *Cont.*

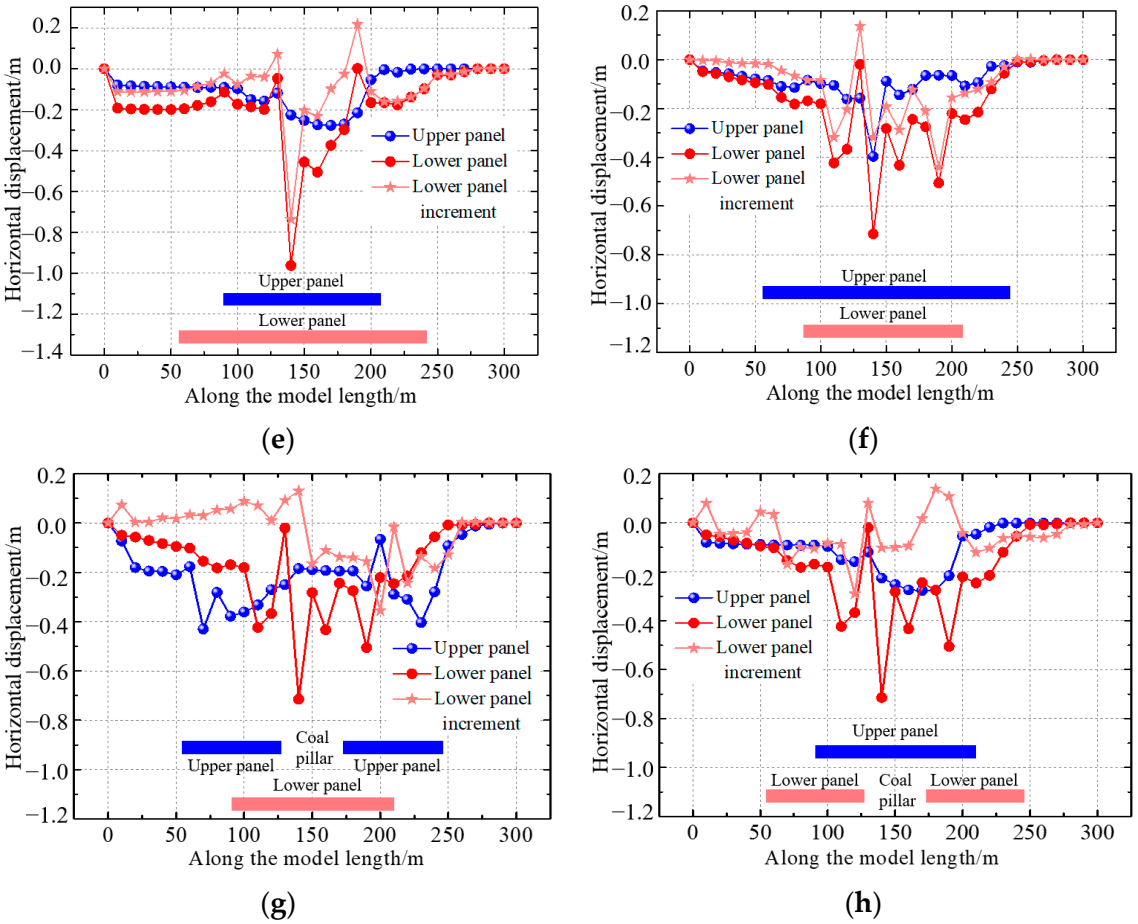

Figure 5. Horizontal displacement of different mining panel layout configurations: (**a**) stacked; (**b**) external staggered; (**c**) the edge of the upper panel, internal staggered; (**d**) the edge of the lower panel internal staggered; (**e**) two edges of the upper panel internal staggered; (**f**) two edges of the lower panel internal staggered; (**g**) external staggered of the upper panel with a coal pillar; (**h**) internal staggered of the upper panel with a coal pillar.

3.3.1. Stacked

The maximum value of horizontal displacement was −0.275 m after the upper panel was extracted. The profile of horizontal displacement became deeper and steeper, and the maximum value increased to −1.335 m. It can be concluded that repeated mining significantly increased the horizontal displacement.

3.3.2. External Staggered

After extracting the upper panel, the maximum value of horizontal displacement was −0.309 m, which was distributed in the overlapped region between the upper and lower panels. The maximum value of horizontal displacement was −0.476 m, which was distributed on the ground surface above the left edge of the lower panel. The other peak value was −0.428 m, located in the overlapped region. The horizontal displacement of the overlapped region changed significantly.

3.3.3. The Edge of the Upper Panel Internal Staggered

The maximum horizontal displacement was −0.309 m after the upper panel was extracted, and the horizontal displacement profile had two peaks of −0.716 m and −0.625 m, respectively, after the extraction of the lower panel. Compared with the horizontal displacement profile of the upper panel extraction, the profile of the lower panel extraction showed

an obvious fluctuation, indicating that the horizontal movement trend had been enhanced to a certain extent.

3.3.4. The Edge of the Lower Panel Internal Staggered

The maximum value of horizontal displacement was −0.396 m after the upper panel was extracted, with only one peak distribution. After the lower panel was extracted, the maximum value increased from −0.396 m to −0.809 m, with three peak distributions. Furthermore, the profile of horizontal displacement fluctuated significantly.

3.3.5. Two Edges of the Upper Panel Internal Staggered

The maximum value of horizontal displacement was −0.277 m after the upper panel was extracted, with a profile shape of a plate. The maximum value of horizontal displacement was −0.963 m after the lower panel was extracted, with the profile shape of a *V*. The maximum value was distributed in the middle region of the goaf.

3.3.6. Two Edges of the Lower Panel Internal Staggered

There was one peak with a value of −0.397 m for the horizontal displacement after the extraction of the upper panel. When the lower panel was extracted, there were four peak distributions of −0.424 m, −0.715 m, −0.433 m, and −0.505 m. Compared with the two edges of the upper panel internal staggered, the horizontal movement of the ground surface was more obvious. The significant change in horizontal displacement was mainly distributed in the overlapped region, which indicated that the mining superimposed effect had significantly affected the profile of horizontal displacement.

3.3.7. External Staggered of the Upper Panel with a Coal Pillar

The profile of horizontal displacement after upper panel extraction had three peak distributions of −0.431 m, −0.378 m, and −0.404 m, and they were distributed on two edges of the upper panel. The profile of horizontal displacement had four peak distributions of −0.399 m, −0.354 m, −0.422 m, and −0.552 m. The obvious change regions of horizontal displacement were mainly the coal pillar region and the overlapped region.

3.3.8. Internal Staggered of the Upper Panel with a Coal Pillar

After the upper panel was extracted, the profile of horizontal displacement had no obvious peak with a maximum value of 0.276 m. The profile of horizontal displacement had three peak values with −0.262 m, −0.451 m, and −0.369 m after the lower panel was extracted. It can be concluded that the obvious change in horizontal displacement mainly emerged in the stage of lower panel extraction.

3.4. Crack Propagation, Break Angle and Movement Angle

3.4.1. Stacked

The movement angle and break angle are important indicators for evaluating MISS and rock strata movement [49,50]. After the upper panel was extracted, the break angles of the two edges of the upper panel were 46° and 45°, respectively, and the movement angles were 22° and 16°, respectively. The lower panel extraction reactivated existing bedding separations and strata cracks, which had been developed in the stage of upper panel extraction. New bedding separations and strata cracks developed, and most of the bedding separations and strata cracks above the middle region of the panels tended to close under the influence of mining-induced disturbance, then the break angle was reduced to 22°. The crack development of the lower panel tended to spread towards the goaf of the upper panel, and the break angle was reduced to 20°. Because of the superimposed effect, the range of MISS expanded, and the movement angles of the two edges increased to 30° and 26°, respectively.

3.4.2. External Staggered

After the lower panel was extracted, strata cracks and bedding separations above the goaf of the upper panel tended to close. The break angle of the left edge of the upper panel was reduced from 32° to 27°, and the break angle of the right edge was still 29° due to the minor impact of strata movement. Under the significant superimposed effect, the movement angle increased to 30°. The significant incremental degree of rock strata movement occurred above the middle region of the overlapped area instead of above the middle region of the lower goaf. Affected by the existing mining-induced disturbance of the upper panel, the break angle of the lower panel was reduced to 25° and 23°, respectively.

3.4.3. The Edge of the Upper Panel Internal Staggered

The changes in movement angle and break angle are presented in Figure 6c. The break angles of the two edges were 35° and 34°, respectively, after the upper panel was extracted, and the movement angles were 22° and 19°, respectively. It also can be concluded that MISS range development was still asymmetric due to the burial depth of the two edges. The bedding separation and strata crack became closed due to the mining-induced disturbance of lower panel extraction. The break angles of the two edges decreased to 31° and 29°, respectively. The bedding separation and strata crack in the interburden region developed because of lower panel extraction. The break angles of the two edges of the lower panel were 28° and 26°, respectively, and the movement angles of the two edges were 15° and 12°, respectively.

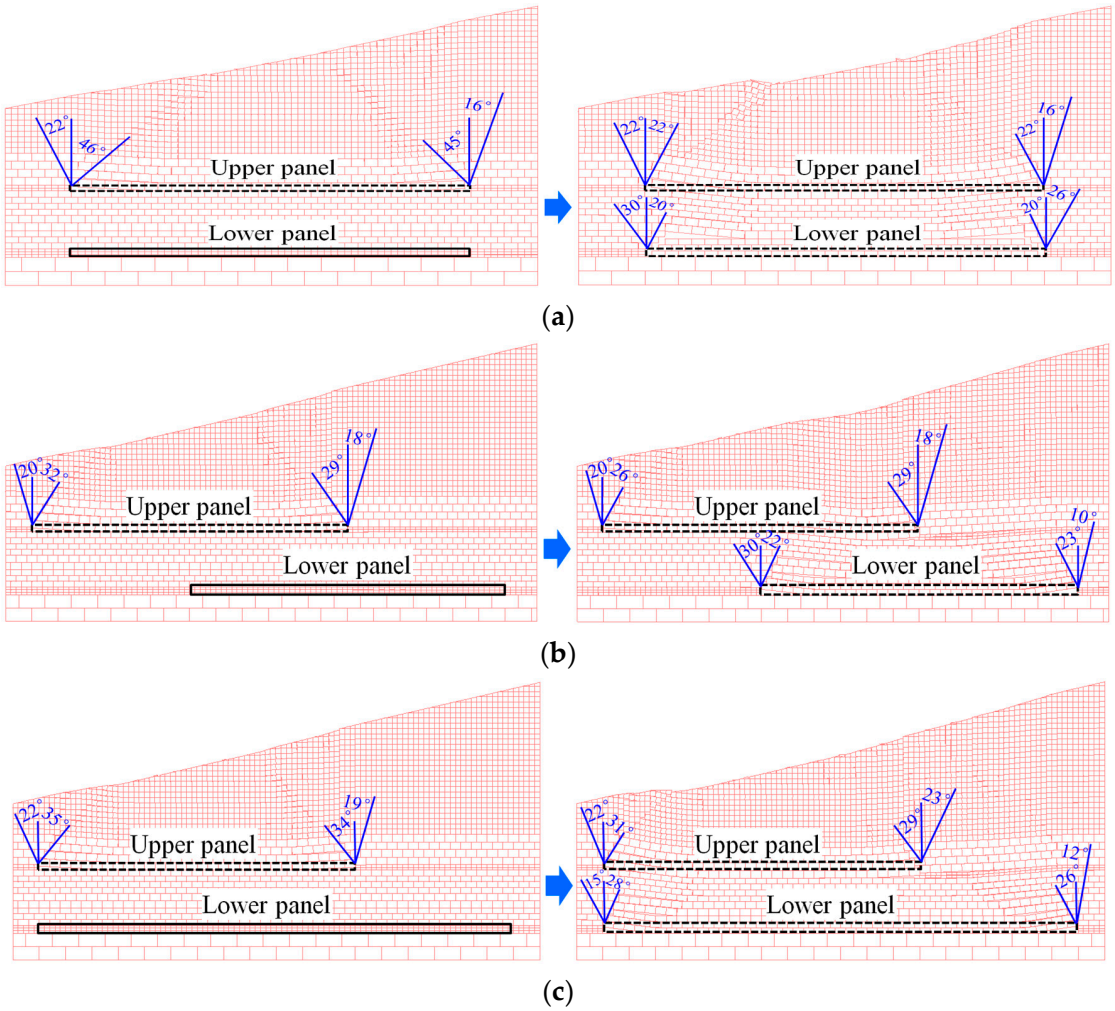

Figure 6. *Cont.*

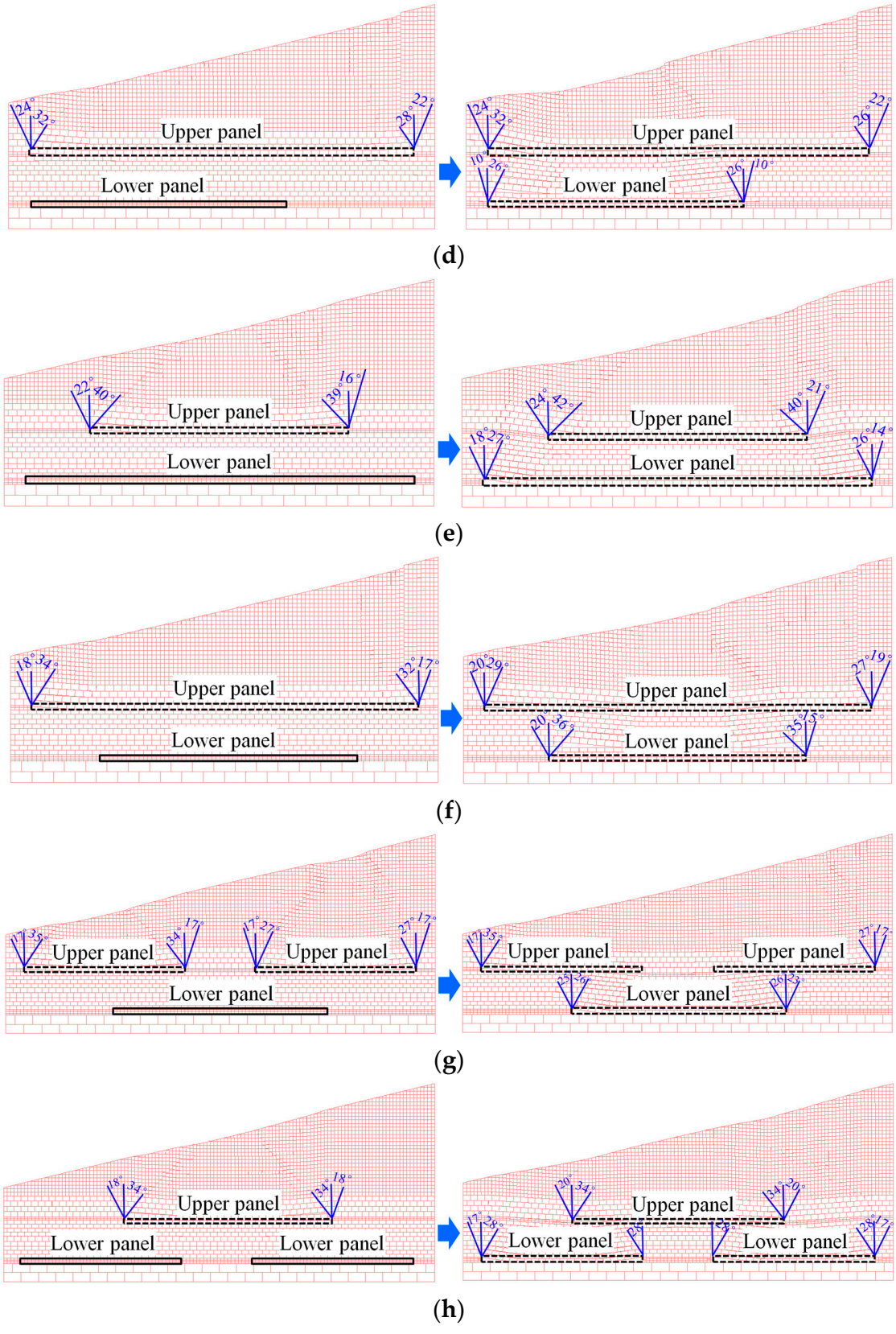

Figure 6. Movement angle and break angle of different mining panel layout configurations: (**a**) stacked; (**b**) external staggered; (**c**) the edge of the upper panel, internal staggered; (**d**) the edge of the lower panel internal staggered; (**e**) two edges of the upper panel internal staggered; (**f**) two edges of the lower panel internal staggered; (**g**) external staggered of the upper panel with a coal pillar; (**h**) internal staggered of the upper panel with a coal pillar.

3.4.4. The Edge of the Lower Panel Internal Staggered

The break angles of two edges of the upper panel were 32° and 28°, respectively, and the movement angles were 24° and 22°, respectively, after the upper panel was extracted. The bedding separation and strata crack development of the upper panel extraction became closed due to mining which was induced by the lower panel extraction, especially in the overlapped region. The MISS became aggravated because of more extraction space. However, the bedding separation and strata crack still kept the previous state of the upper panel extraction. Compared with the upper panel extraction, the break angle and movement angle decreased.

3.4.5. Two Edges of the Upper Panel Internal Staggered

The change in movement angle and break angle is shown in Figure 6e. The break angles of the two edges for upper panel extraction were 40° and 39°, respectively, and the movement angles were 22° and 16°, respectively. The break angle indicated that the MISS range caused by upper panel mining was relatively small. After the lower panel was extracted, the break angles were 27° and 26°, respectively. The bedding separation and strata crack mainly closed in the middle region of the overlap, and then the corresponding movement angles decreased to 18° and 14°, respectively.

3.4.6. External Staggered of the Upper Panel with a Coal Pillar

The change in movement angle and break angle is shown in Figure 6g. Compared with upper panel extraction, the movement angle slightly increased due to an increase in MISS degree. The strata movements after lower panel extraction mainly occurred in the previously disturbed area of upper panel extraction. Unlike other mining layouts, the lower panel did not change the break angle of the two edges for upper panel extraction. The break angle of lower panel extraction slightly decreased to 26°. Due to lower panel extraction, the range of the MISS effect was correspondingly increased, and then the movement angle increased to 25° and 26°, respectively.

3.4.7. Internal Staggered of the Upper Panel with a Coal Pillar

Compared to the external staggered of the upper panel with the coal pillar, after the upper panel was extracted, the movement angle slightly increased. The strata movement, the close and reactive bedding separation, and strata cracks mainly developed in the overlapped region. The break angle of the lower panel extraction decreased to 28°.

3.5. Ground Surface Fissure Development

Ground surface fissures (GSFs) were a direct reflection of the comprehensive effect of overburden movement and surface subsidence on surface damage. GSF development was affected by various mining geological factors such as topsoil layer deformation, overburden movement, and mining-induced subsidence [51–53]. GSF development after lower panel extraction was presented in Figure 6.

3.5.1. Stacked

The stacked configuration has significantly increased the horizontal displacement of the ground surface. GSF development was not obvious after upper panel extraction, and the dimension was slight. One stepped ground fissure was developed on the ground surface above the right edge of the upper panel, and the width and fall were 0.12 m and 0.18 m, respectively. After the lower panel was extracted, three GSFs were developed (Figure 7a). GSF1, with the shape of a *V*, was developed on the ground surface above the left edge of the lower goaf, and its width and fall were 0.41 m and 0.73 m, respectively. On the ground surface above the right edge of the lower goaf, GSF2 and GSF3 were developed. GSF2 was the slided type, and the width, fall, and depth were 0.36 m, 0.3 m, and 13.4 m, respectively. GSF3 was the stepped type, and its fall was 0.75 m. It can be concluded that the GSFs mainly developed on the ground surface above the edge of the goaf.

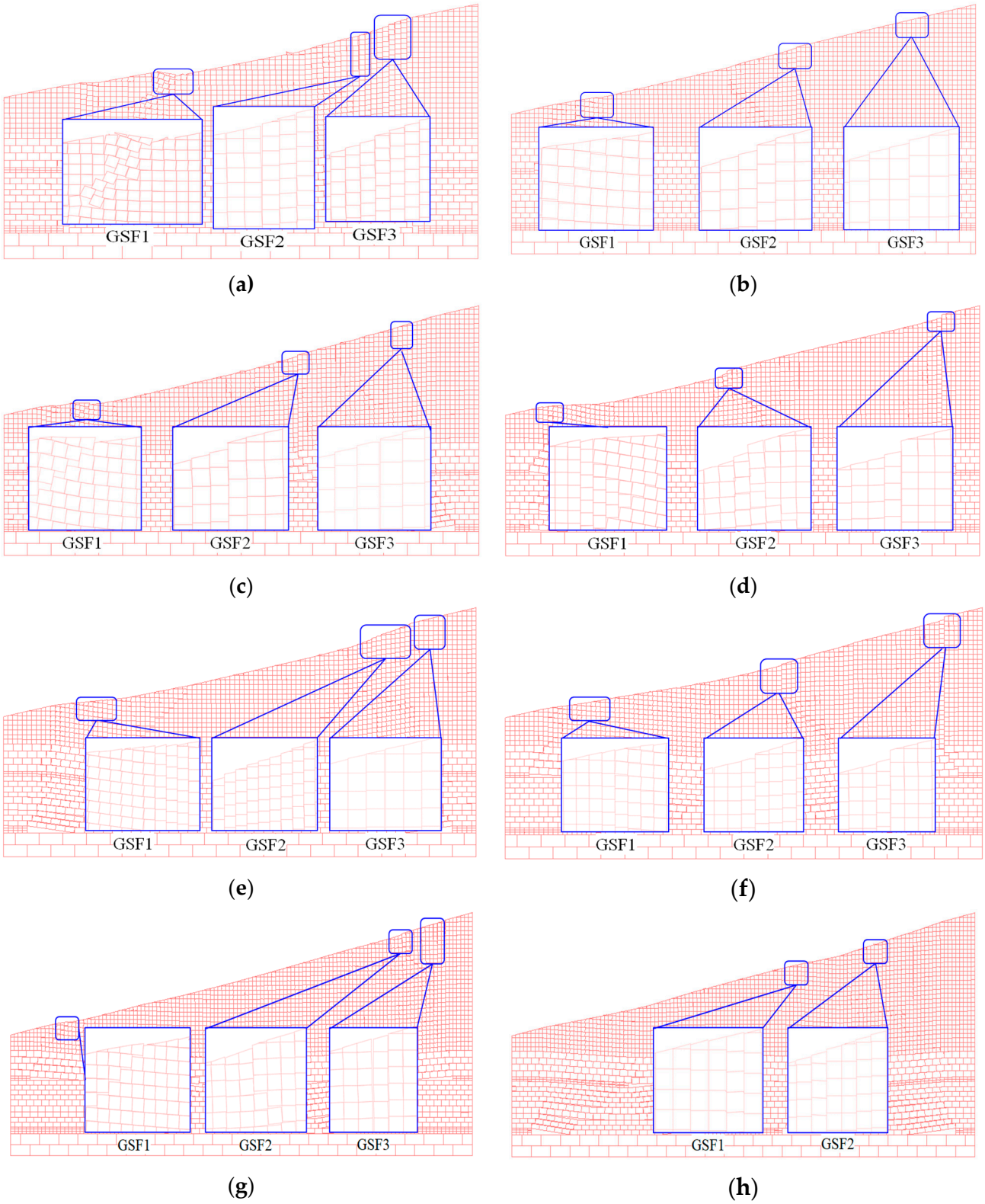

Figure 7. Ground surface fissure development of different mining panel layout configurations: (**a**) stacked; (**b**) external staggered; (**c**) the edge of the upper panel, internal staggered; (**d**) the edge of the lower panel internal staggered; (**e**) two edges of the upper panel internal staggered; (**f**) two edges of the lower panel internal staggered; (**g**) external staggered of the upper panel with a coal pillar; (**h**) internal staggered of the upper panel with a coal pillar.

3.5.2. External Staggered

Three GSFs were developed during the lower extraction stage. GSF1, with the shape of a V, was developed on the ground surface above the upper goaf, and its fall was about 0.2 m. GSF2 was developed on the ground surface above the right edge of the overlapped region, with a fall increasing 0.5 m to 0.63 m. GSF3 was developed on the ground surface above the right edge of the panel, with a width and depth of 0.12 m and 9.5 m, respectively.

3.5.3. The Edge of the Upper Panel Internal Staggered

After the upper panel was extracted, GSF1 with stepped type and a fall of 0.21 m was developed; its fall increased from 0.21 m to 0.72 m, and the topsoil had an obvious dislocation. GSF2 was developed on the ground surface above the right edge of the upper goaf, and the fall significantly increased to 0.7 m. The development shape of GSF3 was slided type, and the width, the fall, and the depth were 0.2 m, 0.224 m, and 7.7 m, respectively.

3.5.4. The Edge of the Lower Panel Internal Staggered

Three GSFs with stepped types were developed after the lower panel was extracted, and the falls of GSF1, GSF2, and GSF3 were 0.4 m, 1.0 m, and 1.3 m, respectively. It should be noted that one GSF with slided type was developed near GSF2, and its width and depth were 0.2 m and 3.5 m, respectively.

3.5.5. Two Edges of the Upper Panel Internal Staggered

The distorted deformation occurred in the rock mass underlying GSF1, and the fall of GSF1 was 0.38 m. A series of GSFs with stepped type were developed on the ground surface above the right edge of the lower panel, and the maximum fall of the stepped fissures was 0.75 m. Additionally, one GSF3 with slided type was developed near GSF2; the width and depth were 0.14 m and 12.5 m, respectively.

3.5.6. Two Edges of the Lower Panel Internal Staggered

After the lower panel was extracted, GSF1 changed slightly; the fall increased from 0.1 m to 0.2 m, and the underlying rock mass shifted to a certain extent. GSF2 was developed on the ground surface above the left edge of the upper goaf, and the fall was still 1.3 m. GSF3 was developed on the ground surface above the right edge of the lower panel. Due to the distorted separation of the rock mass, the fall increased from 1.0 m to 1.3 m.

3.5.7. External Staggered of the Upper Panel with a Coal Pillar

Two GSFs with stepped types and one GSF with a slided type were developed. The falls of GSF1 and GSF2 were 0.3 m and 0.4 m, respectively. GSF3, with a width of 0.34 m and a depth of 13.5 m, was developed on the ground surface above the right edge of the upper goaf. It can be concluded that the development scale of the GSF was not obvious.

3.5.8. Internal Staggered of the Upper Panel with a Coal Pillar

GSF1 with stepped type was developed on the ground surface 38 m away from the right edge of the upper goaf, and the fall was only 0.1 m. After the lower panel was extracted, the fall increased from 0.1 m to 0.16 m. GSF2 was developed on the ground surface above the right edge of the upper goaf, and its type was stepped with a fall of 0.22 m. It can be concluded that this configuration effectively reduced the development scale of GSF and weakened the MISS.

4. Comparative Analysis of MISS with Different Mining Panel Layout Configurations

It can be ascertained that different mining panel layout configurations have different effects on MISS and ground surface damage. In order to determine the preferred mining panel layout configuration, it is necessary to implement a comprehensive analysis from the

perspectives of MISS influence range, ground surface movement, and GSF development scale in order to provide a reliable basis for optimizing the mining system layout.

4.1. MISS Influence Range

The comparison of the influence range of MISS is presented in Table 3. The superimposed effect was significant, and the subsidence coefficient was 0.998, indicating the most serious degree of MISS. The subsidence coefficient of external staggered and internal staggered was 0.847; however, the MISS degree in the overlapped region was significantly increased, while it was not obvious in other regions. Compared with other mining panel layout configurations, the subsidence coefficient of the external staggered of the upper panel with a coal pillar and the internal staggered of the upper panel with a coal pillar were 0.721 and 0.65, respectively. This indicated that these two layout configurations could effectively reduce the degree of MISS.

Table 3. Comparison of MISS influence range.

Mining Panel Layout Configuration	MISS Influence Range	MISS Profile	Break Angle	Movement Angle
Stacked	Subsidence coefficient was 0.998.	The profile presented a V shape and became steep on both edges, and the bottom presented the shape of a bowl.	Significantly decreased from 45° to 20°.	Slightly increased
External staggered (Internal staggered)	MISS of the overlapped region was significantly increased, and the subsidence coefficient was 0.847.	The left part of the profile presented the shape of a plate, and the right part presented a V shape.	Slightly decreased	Slightly increased
The edge of the upper panel internal staggered	MISS of the overlapped region was significantly increased, and the subsidence coefficient was 0.991.	The profile presented a U shape and became steep on both edges, and the bottom presented the shape of a plate.	Slightly decreased	Slightly decreased
The edge of the lower panel internal staggered	MISS of the overlapped region was significantly increased, and the subsidence coefficient was 0.992.	The left part of the profile presented a V shape, and the right part presented the shape of a plate.	Slightly decreased	Slightly decreased
Two edges of the upper panel internal staggered	MISS was serious, and subsidence coefficient was 0.996.	The profile presented a U shape, and the bottom presented the shape of a plate.	Slightly decreased	Slightly decreased
Two edges of the lower panel internal staggered	MISS was serious, and subsidence coefficient was 0.997.	The upper part of the profile presented a U shape, and the lower part presented a V shape.	Slightly decreased	Slightly increased
External staggered of the upper panel with a coal pillar	Subsidence coefficient was 0.721.	The profile presented the shape of a bowl.	Slightly decreased	Slightly increased
Internal staggered of the upper panel with a coal pillar	Subsidence coefficient was 0.65.	The profile presented a W shape.	Slightly decreased	Slightly increased

In terms of the mining development profile, the stacked profile presented a V shape, indicating that the mining degree was concentrated, but the range of full mining was not large. The profile of the overlapped region for external and internal staggered presented a V shape, and the mining degree of the overlapped region was significantly increased. Compared with other mining layout configurations, the mining degree of the external

staggered of the upper panel with a coal pillar and the internal staggered of the upper panel with a coal pillar was relatively weak. From the perspective of break angle and movement angle, upper mining-induced disturbances reduced the mechanical strength of the overlying strata. When affected by the repeated mining of the lower panel extraction, the mechanical strength of the overlying strata was further reduced, resulting in a more obvious mining superimposed effect. Therefore, the break angle of the upper panel mining slightly decreased, while the movement angle slightly increased after the lower panel was extracted. On the basis of the reduction in the overburden mechanical strength and the effect of repeated mining, the break angle was slightly decreased, and the movement angle was slightly increased, indicating that the mining superimposed effect had effectively expanded the mining range.

4.2. Ground Surface Movement

Ground surface movement of different mining layouts is shown in Figure 8. The maximum ground subsidence of stacked, external stacked, the edge of the upper panel internal staggered, and the edge of the lower panel internal staggered were −4.993 m, −4.237 m, −4.958 m, and −4.961 m (Figure 8a), respectively; while the maximum ground subsidence of two edges of the upper panel internal staggered, two edges of the lower panel internal staggered, external staggered of the upper panel with a coal pillar, and internal staggered of the upper panel with a coal pillar were −4.982 m, −4.985 m, −3.607 m, and −3.252 m (Figure 8a), respectively.

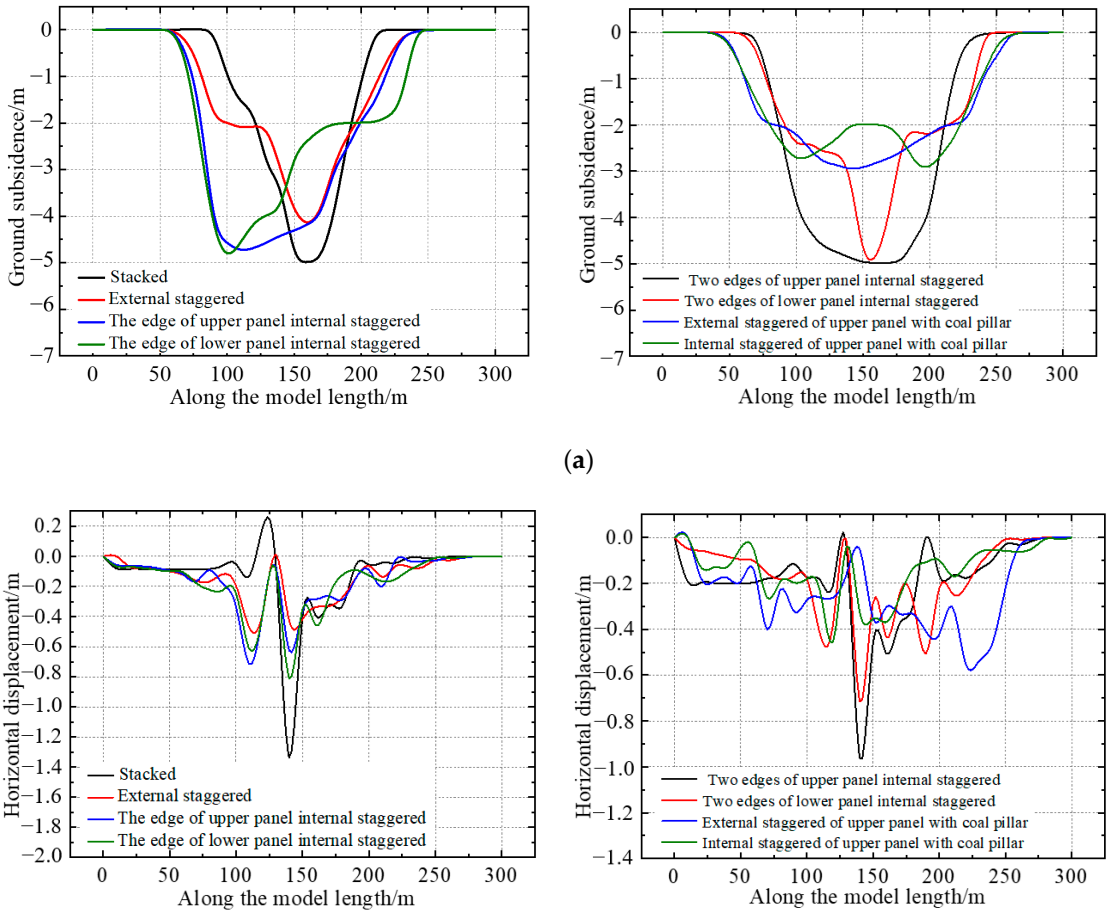

Figure 8. Ground surface movement of different mining layout configurations: (**a**) ground surface subsidence of different mining layout configurations; (**b**) horizontal displacement of different mining layout configurations.

Compared with other mining layout configurations, the MISS profile of the external staggered (internal staggered) of the upper panel with a coal pillar was more gentle, and the MISS degree was weaker. The peak values of horizontal displacement of stacked, external stacked, the edge of upper panel internal staggered, and the edge of the lower panel internal staggered were −1.335 m, −0.4755 m, −0.716 m, and −0.8092 m (Figure 8b), respectively. The peak values of horizontal displacement of two edges of the upper panel internal staggered, two edges of the lower panel internal staggered, external staggered of the upper panel with a coal pillar, and internal staggered of the upper panel with a coal pillar were −0.963 m, −0.7151 m, −0.716 m, and −0.5524 m (Figure 8b), respectively. It can be concluded that the horizontal displacement of the external staggered (internal staggered) of the upper panel with a coal pillar was smaller compared to other layout configurations.

4.3. Ground Surface Fissure Development

The ground surface fissure development scale of different mining layout configurations is presented in Table 4. The numerical simulation results indicated that the development types of GSFs were mostly stepped type, slided type, and graben type in the mining process. It should be highlighted that the development location of a GSF was mainly on the ground surface above the edge of the goaf. In view of the development scale, the GSF fall of stacked, the edge of lower panel internal staggered, two edges of upper panel internal staggered, and two edges of lower panel internal staggered were greater than 0.75 m, and some even were 1.35 m. It indicated that the development scale of these four mining layout configurations was relatively large, and the ground surface damage was obvious. The development fall of the other four mining layout configurations ranged from 0.2 m to 0.4 m. In addition, the maximum fall of the internal staggered (external staggered) of the upper panel with a coal pillar was 0.4 m. In view of the ground surface fissure development, the internal staggered (external staggered) of the upper panel with a coal pillar had slight affection.

Table 4. Comparison of ground fissure development scales of different mining panel layout configurations.

Mining Panel Layout Configuration	The Development Type	The Development Scale	Notes
Stacked	GSF1: Graben GSF2: Slided GSF3: Stepped	GSF1: 0.41 m (width), 0.73 m (fall) GSF2: 0.36 m (width), 0.3 m (fall), and 13.4 m (depth) GSF3: 0.75 m (fall)	
External staggered (Internal staggered)	GSF1: V shape GSF2: Stepped GSF3: Slided	GSF1: 0.21 m (fall) GSF2: 0.5 m → 0.63 m (fall) GSF3: 0.12 m (depth), 9.5 m (depth)	GSF3 was developed after the lower panel was extracted.
The edge of the upper panel internal staggered	GSF1: Stepped GSF2: Stepped GSF3: Slided	GSF1: 0.21 m → 0.72 m (fall) GSF2: 0.7 m (fall) GSF3: 0.2 m (width), 0.224 m (fall), 7.7 m (depth)	GSF3 was developed after the lower panel was extracted.
The edge of the lower panel internal staggered	GSF1: Stepped GSF2: Stepped GSF3: Stepped	GSF1: 0.4 m (fall) GSF2: 1.0 m (fall) GSF3: 1.3 m (fall)	GSF3 was developed after the lower panel was extracted.
Two edges of the upper panel internal staggered	GSF1: Stepped GSF2: Stepped GSF2: Slided	GSF1: 0.38 m (fall) GSF2: 0.75 m (fall) GSF3: 0.14 m (width), 12.5 m (depth)	

Table 4. *Cont.*

Mining Panel Layout Configuration	The Development Type	The Development Scale	Notes
Two edges of the lower panel internal staggered	GSF1: Stepped GSF2: Stepped GSF2: Stepped	GSF1: 0.1 m → 0.2 m (fall) GSF2: 1.3 m (fall) GSF3: 1.0 m → 1.3 m (fall)	
External staggered of the upper panel with a coal pillar	GSF1: Stepped GSF2: Stepped GSF2: Slided	GSF1: 0.3 m (fall) GSF2: 0.4 m (fall) GSF3: 0.34 m (width), 13.5 m (depth)	
Internal staggered of the upper panel with a coal pillar	GSF1: Stepped GSF2: Stepped GSF2: Slided	GSF1: 0.1 m (fall) GSF2: 0.1 m → 0.16 m (fall)	

A comparison of ground fissure development scales of different mining panel layout configurations is shown in Table 4. The numerical simulation results indicated that the development types of ground fissures were mainly stepped and slided. GSF fall of stacked, the edge of upper panel internal staggered, the edge of the lower panel internal staggered, two edges of the upper panel internal staggered and two edges of the lower panel internal staggered was greater than 0.7 m, and some even as great as 1.3 m, indicating that the development scale of GSF of these four mining layout configurations was large, and the mining damage to the surface was relatively obvious. GSF fall of external staggered, internal staggered, and external staggered of the upper panel with a coal pillar ranged from 0.3 m to 0.63 m, and the GSF fall of the internal staggered of the upper panel with a coal pillar was only 0.16 m, indicating this mining layout configuration had the minimum effect on the ground surface.

5. Discussion

This study presented the surface subsidence characteristics of different mining panel layout configurations with multi-seam longwall mining. The mining panel layout configurations were proposed. Thus, ground surface subsidence, horizontal displacement, crack propagation, break angle, movement angle, and ground fissure development were investigated by numerical simulation method. After the comparison of different mining panel layout configurations, the preferred mining panel layout mode, such as the external staggered (internal staggered) and external staggered (internal staggered) of the upper panel with a coal pillar, was determined. These four mining layout configurations should be preferred according to the overall layout of mining-induced excavation.

The mining panel layout configuration has a significant impact on the surface subsidence degree, especially under the condition of multi-seam mining. Multi-seam mining has a significant impact on each other, but few studies have been conducted considering the mining panel layout configuration. In addition, obtaining rich data through field measurement typically consume considerable time and effort. Hence, in order to explore the characteristics of surface subsidence, numerical simulation can be a preferred research method in this study. The numerical simulation results are not as accurate as field measurement results, but they can reflect the changing trend of surface subsidence. The field measurement results and numerical simulation results can be mutually verified, which will enrich relevant achievements.

Under the condition of multi-seam mining, the stress concentration induced by the coal pillar has a significant impact on coal seam safety extraction, especially concerning the coal seam extraction condition of coal and gas outburst. Considering that the coal pillar reserved in the upper panel would bring some difficulties to the gas control of the lower mining panel, an external staggered upper panel with a coal pillar was more suitable for field engineering practice. It should be noted that the stress concentration requires early pressure relief. In order to maximize the resource recovery rate, the external staggered (internal

staggered) configuration can be selected as the working face deployment configuration. Due to the different occurrence conditions of mining geology, one or several working face mining panel layout configurations should be selected based on the consideration of the mining geological environment. In order to achieve an orderly connection of the mining progress, the mining panel layout configuration should also be considered from the design of the mining area, and the overall excavation plan should be determined. Moreover, detailed parameters of the upper coal seam, lower coal seam, and coal pillar should be explored in future studies.

6. Conclusions

The multi-seam surface subsidence profile has its special features. The relative location of mining panels in two seams has an important influence on the changes in subsidence profile, crack propagation, and ground surface fissure development. This phenomenon has been investigated through numerical simulation. In order to study the multi-seam subsidence characteristics because of different mining configurations, the numerical simulation parameters were kept constant in all models. The results indicated that in the overlapped region of the upper and lower panels, the existing bedding separations and strata cracks closed and activated, reducing the bearing capacity of previously disturbed strata. Correspondingly, the subsidence magnitude increased. The subsidence profile became steeper and deeper for stacked configuration, while the subsidence magnitude of external staggering of the upper panel with a coal pillar and internal staggering of the upper panel with a coal pillar was slight due to the support action of the reserved coal pillar.

The type of ground surface fissure was mainly stepped and slided, developed on the ground surface above the edge of the mining panel, and its location was closely associated with the edge of the strata movement. Compared to the range of subsidence influence, ground surface movement, and ground surface fissure development, the external staggered (internal staggered) and external staggered (internal staggered) of the upper panel with a coal pillar can be preferred as the mining layout configuration. In terms of recovery rate, the configuration of external staggered (internal staggered) can be applied in engineering practice.

The significance of this study is that the surface subsidence characteristics can be applied to determine the effect of different mining layout configurations on surface subsidence. Combined with specific parameters, it can be used to assess the influence of different mining panel layout configurations on the ground surface. In addition, the surface subsidence features of different mining layout configurations can contribute to the prediction methods.

Author Contributions: Conceptualization, H.Z. and H.W.; Methodology, H.Z.; Validation, H.Z., H.W., R.G. and Y.Z.; Formal analysis, H.Z.; Investigation, H.Z., H.W., R.G. and Y.Z.; Data curation, H.Z.; Writing—original draft, H.Z.; Writing—review and editing, H.Z.; Visualization, H.Z.; Supervision, H.W. All authors have read and agreed to the published version of the manuscript.

Funding: This study is supported by the Open Fund of State Key Laboratory of Water Resource Protection and Utilization in Coal Mining (WPUKFJJ2019-19), Major research project of Guizhou Provincial Department of Education on innovative groups (Qianjiaohe KY [2019] 070), State Key Laboratory of Strata Intelligent Control and Green Mining Co-founded by Shandong Province and the Ministry of Science and Technology, Shandong University of Science and Technology (MDPC2023ZR01; No. SICGM202203).

Data Availability Statement: The data used to support the findings of this research are included in the paper.

Acknowledgments: All authors thank the editor and anonymous reviewers for their constructive comments and suggestions to improve the quality of this paper.

Conflicts of Interest: The authors declare no conflict of interest.

References

1. Peng, S.S. *Surface Subsidence Engineering*; SME: New York, USA, 1992.
2. Jiránková, E.; Waclawik, P.; Nemcik, J. Assessment of models to predict surface subsidence in the Czech part of the Upper Silesian Coal Basin—Case study. *Acta Geodyn. Et Geomater.* **2020**, *17*, 469–484. [CrossRef]
3. Zhu, H.Z.; He, F.L.; Zhang, S.B.; Yang, Z.Q. An integrated treatment technology for ground fissures of shallow coal seam mining in the mountainous area of southwestern China: A typical case study. *Gospod. Surowcami Miner.-Miner. Resour. Manag.* **2018**, *34*, 119–137.
4. Tajduś, K.; Misa, R.; Sroka, A. Analysis of the surface horizontal displacement changes due to longwall panel advance. *Int. J. Rock Mech. Min. Sci.* **2018**, *104*, 119–125. [CrossRef]
5. Tichavský, R.; Jiránková, E.; Fabiánová, A. Dating of mining-induced subsidence based on a combination of dendrogeomorphic methods and in situ monitoring. *Eng. Geol.* **2020**, *272*, 105650. [CrossRef]
6. Booth, C.J.; Curtiss, A.M.; Demaris, P.J.; Van Roosendaal, D.J. Anomalous increases in piezometric levels in advance of longwall mining subsidence. *Environ. Eng. Geosci.* **1999**, *5*, 407–417. [CrossRef]
7. Mao, G.Z.; Fan, Y.; Li, X.S.; Ou, J.E.; Fang, X.R.; Zhu, H.M.; He, P.R. Progress of the studies of mining subsidence: Based on the literature statistics of CNKI journals from 2011 to 2021. *Mod. Min.* **2022**, *38*, 53–57+94.
8. Cui, X.M.; Deng, K.Z. Research review of predicting theory and method for coal mining subsidence. *Coal Sci. Technol.* **2017**, *45*, 160–169.
9. Hejmanowski, R.; Malinowska, A.A. Evaluation of reliability of subsidence prediction based on spatial statistical analysis. *Int. J. Rock Mech. Min. Sci.* **2009**, *46*, 432–438. [CrossRef]
10. Jiang, Y.; Preusse, A.; Sroka, A. *Angewandte Bodenbewegungsund Bergschadenkunde*; VGE Verlag: Essen, Germany, 2006.
11. Keinhorsh, H. Bei Bodensenkungen auftretende bodenverschiebun-gen und bodenspannungen. *Glückauf* **1928**, *64*, 1141–1145.
12. Avershin. Strata movement in underground coal mining. In *Teaching and Research Group of Mine Survey in Beijing Institute of Mining and Technology (Translation)*; Coal Industry Press: Beijing, China, 1959.
13. Perz, F. Der Einfluß der Zeit auf die Bodenbewegung über Abbauen. *Mitt. Marks.* **1948**, *55*, 92–117.
14. Cui, X.M. Prediction of progressive surface subsidence above longwall coal mining using a time function. *Int. J. Rock Mech. Min. Sci.* **2001**, *38*, 1057–1063. [CrossRef]
15. Liu, Y.C.; Cao, S.G.; Liu, Y.B. Discussion on some time functions for describing dynamic course of surface subsidence due to mining. *Rock Soil Mech.* **2010**, *31*, 925–931.
16. Ma, W.M.; Wang, J.Z.; Kratzsch, H. *Mining Damage and Protection*; Coal Industry Press: Beijing, China, 1984.
17. Liu, Y.C. *Study on the Dynamic Course of the Surface Subsidence and the Model Based on Theory of Key Rock Stratum*; Chongqing University: Chongqing, China, 2010.
18. Dai, H.Y.; Li, W.C.; Liu, Y.X.; Jiang, Y.D. Numerical simulation of surface movement laws under different unconsolidated layers thickness. *Trans. Nonferrous Met. Soc. China* **2011**, *21*, 599–603. [CrossRef]
19. Guo, W.B.; Hou, Q.L.; Zou, Y.F. Relationship between surface subsidence factor and mining depth of strip pillar mining. *Trans. Nonferrous Met. Soc. China* **2011**, *21*, 594–598. [CrossRef]
20. Wang, B.L.; Xu, J.L.; Xuan, D.Y. Time function model of dynamic surface subsidence assessment of grout-injected overburden of a coal mine. *Int. J. Rock Mech. Min. Sci.* **2018**, *104*, 1–8. [CrossRef]
21. Sun, Y.J.; Zuo, J.P.; Karakus, M.; Liu, L.; Zhou, H.W.; Yu, M.L. A new theoretical method to predict strata movement and surface subsidence due to inclined coal seam mining. *Rock Mech. Rock Eng.* **2021**, *54*, 2723–2740. [CrossRef]
22. Sun, Y.J.; Zuo, J.P.; Karakus, M.; Wang, J.T. Investigation of movement and damage of integral overburden during shallow coal seam mining. *Int. J. Rock Mech. Min. Sci.* **2019**, *117*, 63–75. [CrossRef]
23. Chi, S.S.; Wang, L.; Yu, X.X.; Lv, W.C.; Fang, X.J. Research on dynamic prediction model of surface subsidence in mining areas with thick unconsolidated layers. *Energy Explor. Exploit.* **2021**, *39*, 927–943. [CrossRef]
24. Zhu, X.J.; Guo, G.L.; Liu, H.; Yang, X.Y. Surface subsidence prediction method of backfill-strip mining in coal mining. *Bull. Eng. Geol. Environ.* **2019**, *78*, 6235–6248. [CrossRef]
25. Yan, W.T.; Chen, J.J.; Yan, Y.G. A new model for predicting surface mining subsidence: The improved lognormal function model. *Geosci. J.* **2018**, *23*, 165–174. [CrossRef]
26. Sidki-Rius, N.; Sanmiquel, L.; Bascompta, M.; Parcerisa, D. Subsidence management and prediction system: A case study in Potash Mining. *Minerals* **2022**, *12*, 1155. [CrossRef]
27. Huang, G.; Pinnaduwa Kulatilake, H.S.W.; Shreedharan, S.; Cai, S.J.; Song, H.Q. 3-D discontinuum numerical modeling of subsidence incorporating ore extraction and backfilling operations in an underground iron mine in china. *Int. J. Min. Sci. Technol.* **2017**, *27*, 191–201. [CrossRef]
28. Pan, R.K.; Li, Y.; Wang, H.; Chen, J.; Xu, Y.L.; Yang, H.Y.; Cao, S.G. A new model for the identification of subcritical surface subsidence in deep pillarless mining. *Eng. Fail. Anal.* **2021**, *129*, 105631. [CrossRef]
29. Ren, J.C.; Kang, X.T.; Tang, M.; Gao, L.; Hu, J.G.; Zhou, C.L. Coal mining surface damage characteristics and restoration technology. *Sustainability* **2022**, *14*, 9745. [CrossRef]
30. Müller, D.; Preusse, A. Use of the area of main influence to fix a relevant boundary for mining damages in Germany. *Int. J. Min. Sci. Technol.* **2018**, *28*, 79–83. [CrossRef]

31. Diao, X.P.; Bai, Z.H.; Wu, K.; Zhou, D.W.; Li, Z.L. Assessment of mining-induced damage to structures using InSAR time series analysis: A case study of Jiulong Mine, China. *Environ. Earth Sci.* **2018**, *77*, 166. [CrossRef]
32. Diao, X.; Wu, K.; Zhou, D.; Wang, J.; Duan, Z.; Yu, Z. Combining subsidence theory and slope stability analysis method for building damage assessment in mountainous mining subsidence regions. *PLoS ONE* **2019**, *14*, e02100212019. [CrossRef]
33. Kim, J.H.; Kim, K.H.; Yoo, S.H. Evaluating and ranking the mining damage prevention programs in South Korea: An application of the fuzzy set theory. *Resour. Policy* **2022**, *78*, 102873. [CrossRef]
34. Nadiri, A.A.; Taheri, Z.; Khatibi, R.; Barzegari, G.; Dideban, K. Introducing a new framework for mapping subsidence vulnerability indices (SVIs): ALPRIFT. *Sci. Total Environ.* **2018**, *628*, 1043–1057. [CrossRef] [PubMed]
35. Nadiri, A.A.; Khatibi, R.; Khalifi, P.; Feizizadeh, B. A study of subsidence hotspots by mapping vulnerability indices through innovatory 'ALPRIFT' using artificial intelligence at two levels. *Bull. Eng. Geol. Environ.* **2020**, *79*, 3989–4003. [CrossRef]
36. Sadeghfam, S.; Khatibi, R.; Dadashi, S.; Nadiri, A.A. Transforming subsidence vulnerability indexing based on ALPRIFT into risk indexing using a new fuzzy-catastrophe scheme. *Environ. Impact Assess. Rev.* **2020**, *82*, 106352. [CrossRef]
37. Gharekhani, M.; Nadiri, A.A.; Khatibi, R.; Sadeghfam, S. An investigation into time-variant subsidence potentials using inclusive multiple modelling strategies. *J. Environ. Manag.* **2021**, *294*, 112949. [CrossRef] [PubMed]
38. Zhang, J.X.; Sun, Q.; Fourie, A.; Ju, F.; Dong, X.J. Risk assessment and prevention of surface subsidence in deep multiple coal seam mining under dense above-ground buildings: Case study. *Hum. Ecol. Risk Assess. Int. J.* **2018**, *25*, 1579–1593. [CrossRef]
39. Yang, D.D.; Qiu, H.J.; Ma, S.Y.; Liu, Z.J.; Du, C.; Zhu, Y.; Cao, M.M. Slow surface subsidence and its impact on shallow loess landslides in a coal mining area. *Catena* **2021**, *209*, 105830. [CrossRef]
40. Li, G.; Steuart, P.; Pquet, R.; Ramage, R. A case study on mine subsidence due to multi seam longwall extraction. In Proceedings of the Second Australasian Ground Control in Mining Conference, Sydney, Australia, 23–24 November 2010; pp. 191–200.
41. Ghabraie, B.; Ghabraie, K.; Ren, G.; Smith, J.V. Numerical modelling of multistage caving processes: Insights from multi-seam longwall mining-induced subsidence. *Int. J. Numer. Anal. Methods Geomech.* **2017**, *41*, 1–17. [CrossRef]
42. Li, G.; Steuart, P.; Pâquet, R. A case study on multi-seam subsidence with specific reference to longwall mining under existing longwall goaf. In Proceedings of the Seventh Triennial Conference on Mine Subsidence, Sydney, Australia, 26–27 November 2007; pp. 111–125.
43. MSEC. North Wambo Underground modification subsidence assessment—Report number MSEC495. *Tech. Rep. Mine Subsid. Eng. Consult.* **2012**.
44. Guo, G.L.; Wang, Y.H.; Ma, Z.G. A new method for ground subsidence control in coal mining. *J. China Univ. Min. Technol.* **2004**, *33*, 26–29.
45. Galvin, J.M. *Ground Engineering Principles and Practices for Underground Coal Mining*, 1st ed.; Springer International Publishing: Cham, Switzerland, 2016.
46. Adhikary, D.; Khanal, M.; Jayasundara, C.; Balusu, R. Deficiencies in 2d simulation: A comparative study of 2d versus 3d simulation of multi-seam longwall mining. *Rock Mech. Rock Eng.* **2015**, *49*, 2181–2185. [CrossRef]
47. Parmar, H.; Yarahmadi Bafghi, A.; Najafi, M. Impact of ground surface subsidence due to underground mining on surface infrastructure: The case of the Anomaly No. 12 Sechahun, Iran. *Environ. Earth Sci.* **2019**, *78*, 1–14. [CrossRef]
48. Suchowerska, A.M. *The Geomechanics of Single-Seam and Multi-Seam Longwall Coal Mining*; University of Newcastle: Newcastle, Australia, 2014.
49. Unlu, T.; Akcin, H.; Yilmaz, O. An integrated approach for the prediction of subsidence for coal mining basins. *Eng. Geol.* **2013**, *166*, 186–203. [CrossRef]
50. Luo, Y.; Qiu, B. CISPM-MS: A tool to predict surface subsidence and to study interactions associated with multi-seam mining operations. In Proceedings of the 31st International Conference on Ground Control in Mining, Morgantown, WV, USA, 31 July–2 August 2012; pp. 1–7.
51. Zhao, K.; Xu, N.; Mei, G.; Tian, H. Predicting the Distribution of Ground Fissures and Water-Conducted Fissures Induced by Coal Mining: A Case Study. *Springerplus* **2016**, *5*, 977. [CrossRef] [PubMed]
52. Liu, N.N.; Feng, X.Y.; Huang, Q.B.; Fan, W.; Peng, J.B.; Lu, Q.Z.; Liu, W.L. Dynamic characteristics of a ground fissure site. *Eng. Geol.* **2019**, *248*, 220–229. [CrossRef]
53. Howard, K.W.F.; Zhou, W.F. Overview of ground fissure research in China. *Environ. Earth Sci.* **2019**, *78*, 97. [CrossRef]